An Acad Bras Cienc (2024) 96(Suppl. 2): e20240573 DOI 10.1590/0001-3765202420240573
Anais da Academia Brasileira de Ciências | *Annals of the Brazilian Academy of Sciences*
Printed ISSN 0001-3765 I Online ISSN 1678-2690
www.scielo.br/aabc | www.fb.com/aabcjournal

GEOSCIENCES

Drivers and fluxes of dissolved organic carbon along the northern Antarctic Peninsula during late summer

RAQUEL AVELINA, LETICIA C. DA CUNHA, RODRIGO KERR, CÁSSIA O. FARIAS, CLAUDIA HAMACHER & MAURICIO M. MATA

Abstract: Dissolved organic carbon (DOC) is a key component of the biogeochemical carbon cycle in the Southern Ocean. However, there are still significant gaps in understanding the role of DOC in polar environments, due to the limitations of spatiotemporal sampling. In this study, we investigated the regional aspects controlling the distribution and diffusive and advective fluxes of DOC along the northern Antarctic Peninsula (NAP) during austral late summers of 1995 and between 2015 and 2019. DOC concentrations ranged from 33.1 to 157.6 μmol kg^{-1}. The NAP showed regional differences in both its hydrographic conditions and DOC distribution. The regional variability reflected the main biogeochemical sources and fates of DOC associated with the Antarctic Circumpolar Current inflows, the Weddell Gyre transport and the meltwater input. The intensity of the advective fluxes of DOC was 10^6 times greater than the diffusive fluxes. However, ocean fronts along NAP environments are mesoscale structures for observations of downward and upward diffusive fluxes of DOC. This study adds insights on the role of DOC as a proxy for a better understanding of the coupling between physical and biogeochemical processes over time in an environment sensitive to climate change.

Key words: biological pump, carbon cycle, diffusive fluxes, advective fluxes, organic matter, Southern Ocean.

INTRODUCTION

The organic carbon (C) pool in the marine environment corresponds to 700 Pg C, encompassing both particulate organic carbon (POC) and dissolved organic carbon (DOC; Friedlingstein et al. 2019, 2023). Approximately 95% of all oceans organic carbon is in the form of DOC, corresponding to a stock of 662 ± 32 Pg C (Hansell et al. 2009). DOC plays a fundamental role in the ocean's biological pump, linking the chemical processes of the global carbon cycle and the metabolic activities of different organisms (Ducklow et al. 1995, Hansell & Carlson 1998b, Ogawa & Tanoue 2003, Reinthaler et al. 2013). DOC is also classified by its labile, semi-labile and refractory fractions (Hansell et al. 2002, Romera-Castillo et al. 2019), which indicate the resistance of the molecules to microbial, photochemical and/or hydrothermal disruption and, consequently, the cycling time of DOC in the oceans (Orellana & Verdugo 2003, Hansell et al. 2009, Lønborg et al. 2020). The unprecedented increase in atmospheric carbon dioxide (CO_2) emissions and global warming may be a determining factor in the production and degradation of DOC over time (Lønborg et al. 2020).

In addition to biogeochemical processes, ocean circulation plays a fundamental role in controlling the advective and convective fluxes that determine the global export of DOC throughout the water column (Doval et al. 2002, Hansell et al. 2002, da Cunha et al. 2018, Avelina et al. 2020). Surface ocean currents transport DOC laterally over long distances, redistributing both allochthonous and autochthonous DOC (Guo et al. 1995, Roshan & DeVries 2017). The export of DOC from the surface to deeper ocean layers also depends on surface convective mixing and diffusive fluxes throughout the water column (Ducklow et al. 2001, Hansell et al. 2002, Roshan & DeVries 2017). For instance, deep and bottom waters can be enriched with DOC during convective processes of water mass formation (Hansell & Carlson 1998a, Bercovici et al. 2017). On the other hand, the molecular diffusion of matter undoes the concentration gradients of the DOC, inducing a net transport from the more concentrated area to the less concentrated one (Guo et al. 1995, Doval et al. 2002, Schafstall et al. 2010, Zhang et al. 2017, Loginova et al. 2018).

The northern Antarctic Peninsula (NAP), a transition zone between subpolar-polar and oceanic-coastal environments (Dotto et al. 2021) and sensitive to climate change (Fabrés et al. 2000, Huneke et al. 2016, Kerr et al. 2018b), is a key scenario for monitoring long-term DOC ocean distributions and internal fluxes. The first study of DOC distributions and fluxes in the NAP took place in 1995, as part of the oceanographic cruise FRUELA (Doval et al. 2002). Although some sampling efforts have been made over the years (e.g. Ruiz-Halpern et al. 2011, 2014), DOC observations along the NAP have still been low. In order to mitigate the gaps in the understanding of the role of DOC in the biogeochemistry of the NAP, the Brazilian High Latitude Oceanography Group (GOAL; Mata et al. 2018) has been carrying out a continuous effort of DOC observations in the NAP since the austral late summer of 2015. Long-term observations of DOC in environments such as the NAP are important for reducing uncertainties about the impacts of climate change on the biogeochemical and carbon cycles of the Southern Ocean (Lønborg et al. 2020, Henley et al. 2020). Therefore, in this study we evaluate the main regional aspects controlling the distribution and diffusive and advective fluxes of DOC along the NAP during the austral late summer, considering the FRUELA 1995 data (Doval et al. 2002) and the GOAL dataset collected between 2015 and 2019.

Oceanographic features of the northern Antarctic Peninsula

The NAP encompasses the southernmost Drake Passage, the Bellingshausen Sea, the Gerlache Strait, the Bransfield Strait and the western Weddell Sea (Figure 1; Kerr et al. 2018b, Dotto et al. 2021). The ocean circulation along the NAP depends on the Antarctic Circumpolar Current (ACC) and its fronts near the southernmost Drake Passage (Figure 1), respectively the Southern ACC Front (SACCF) and the Southern Boundary of the ACC (SBdy; Orsi et al. 1995). Along the Bransfield Strait, an area of complex circulation and mixing of water masses in the NAP (García et al. 2002, Sangrà et al. 2011, Damini et al. 2022), there are two ocean fronts (Figure 1): (i) the Bransfield Front, which is positioned in the subsurface and linked to the Bransfield Current, close to the southern continental margin of the South Shetland Islands and; (ii) the Peninsula Front, which is positioned close to the Antarctic Peninsula, from surface to 100 m, approximately (Sangrà et al. 2011, 2017).

The NAP environments are impacted by still unknown frequency of intrusions of Circumpolar Deep Water (CDW) from the Bellingshausen Sea and advection of Dense Shelf Water (DSW) from the Weddell Sea (Ruiz Barlett et al. 2018, Damini et al. 2022). The influx of meltwater also has a significant

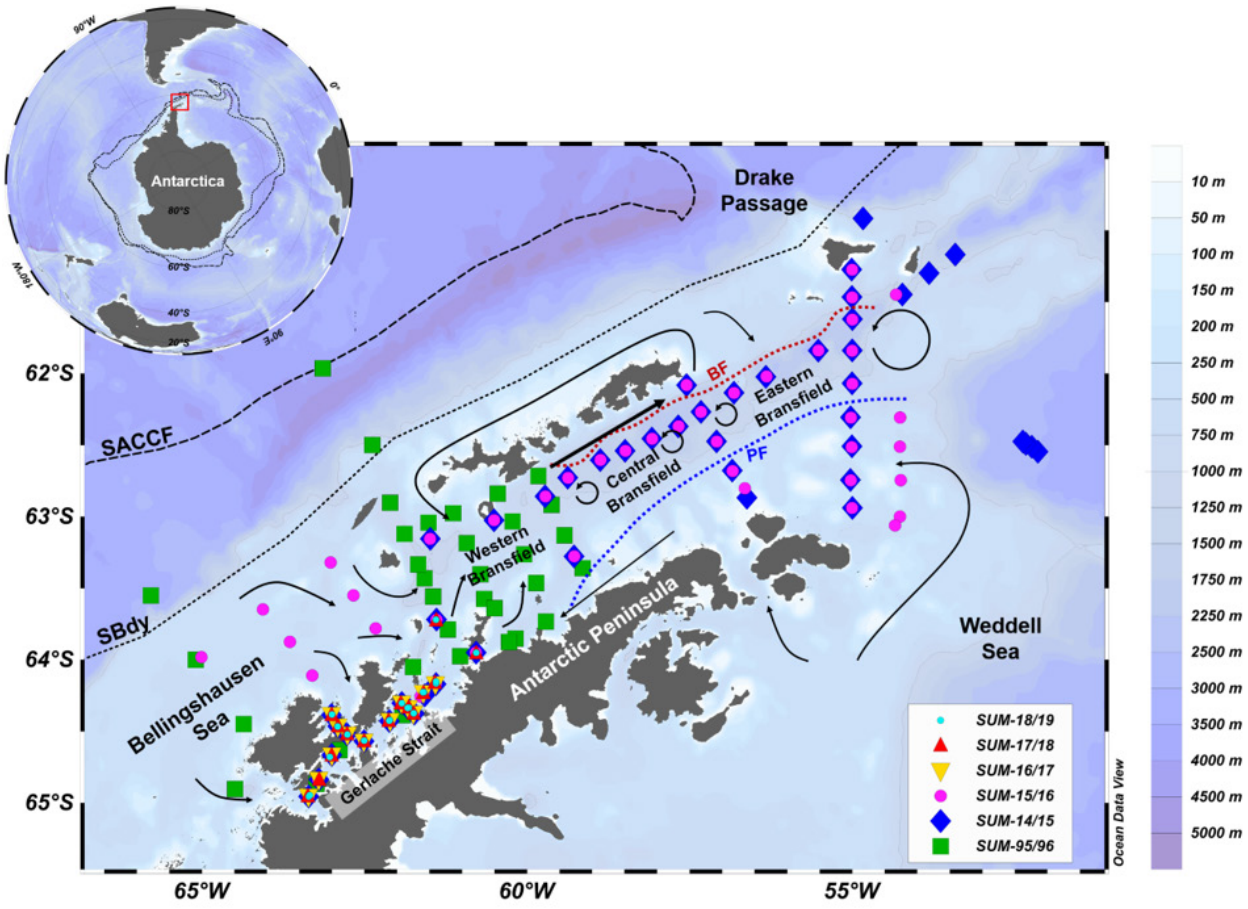

Figure 1. **Map of Antarctica and the northern Antarctic Peninsula (NAP) and location of oceanographic stations carried out during the oceanographic cruises evaluated in this study. The red rectangle corresponds to the NAP area. The symbols correspond to the oceanographic cruises: FRUELA, SUM-95/96 (green square; Doval et al. 2002, Hansell et al. 2021) and the NAUTILUS cruises, respectively, SUM-14/15 (blue diamond), SUM-15/16 (pink circle), SUM-16/17 (yellow inverted triangle), SUM-17/18 (red triangle) and SUM-18/19 (light blue dot). Dashed and dotted black lines correspond, respectively, to the Southern Antarctic Circumpolar Current Front (SACCF), the Southern Boundary of the ACC (SBdy; Orsi et al. 1995). The red and blue dotted lines correspond, respectively, to the Bransfield Front (BF) and Peninsula Front (PF). Black arrows correspond to the location in the NAP (Sangrà et al. 2011, 2017, Dotto et al. 2016). Map created using Ocean Data View software (Schlitzer 2024).**

impact on the region (Loeb et al. 2010). The modified CDW (mCDW) is a relatively warm, salty and poor-oxygenated water mass formed by the mixing of the CDW (temperatures > 1°C and dissolved oxygen concentrations < 225 µmol kg^{-1}) with the colder, low-salinity coastal and shelf waters present in the NAP (Ruiz Barlett et al. 2018, Santos-Andrade et al. 2023). DSW refers to a combination of shelf water varieties, i.e. High-Salinity Shelf Water (HSSW) and Low-Salinity Shelf Water (LSSW), recently ventilated along the Weddell Sea western shelf with temperatures below –1°C and high dissolved oxygen concentrations (> 225 µmol kg^{-1}; Dotto et al. 2016, Ruiz Barlett et al. 2018, Santos-Andrade et al. 2023).

The volumes of mCDW and DSW observed along the NAP can be modified due to the variability of the large-scale climate modes El Niño – Southern Oscillation (ENSO) and the Southern Annular Mode (SAM; Dotto et al. 2016, Ruiz Barlett et al. 2018, Damini et al. 2022, Santos-Andrade et al. 2023).

Higher mCDW intrusions are related to periods of positive SAM due to intensification of westerly winds and/or negative ENSO, when the ACC is strengthened (Loeb et al. 2009, Dotto et al. 2016, Damini et al. 2022, Santos-Andrade et al. 2023). In contrast, greater inputs of DSW can occur during negative SAM events, due to the weakening of westerly winds and/or positive ENSO, due to the intensification of the Weddell Gyre (Loeb et al. 2009, Dotto et al. 2016, Damini et al. 2022, Santos-Andrade et al. 2023).

MATERIALS AND METHODS

Study area and sampling strategy

The study area encompassed the coastal and ocean regions of the NAP (Kerr et al. 2018b, Dotto et al. 2021). The Bransfield Strait has been subdivided into its western, central, and eastern basins. The oceanographic stations were distributed between latitudes 60.9°S and 65°S and longitudes 62.4°W and 65.8°W (Figure 1).

The hydrographic data set (i.e. potential temperature, practical salinity, and potential density) and DOC data analyzed in this study included data from the FRUELA 1995 cruise (Anadón & Estrada 2002, Doval et al. 2002) available in DOM Compilation v2.2021 (Hansell et al. 2021) as well as the GOAL dataset obtained during the NAUTILUS project in five consecutive austral late summers between 2015 and 2019 (Table I). This study revisited the datasets for the Gerlache Strait (da Cunha et al. 2018) and Bransfield Strait (Avelina et al. 2020) obtained between 2015 and 2016 and presents unpublished results sampled by GOAL in 2015 and 2016 in the southernmost Drake Passage and the Bellingshausen and Weddell Seas as well as the dataset from the Gerlache Strait collected in 2017, 2018 and 2019. All DOC datasets from the NAUTILUS cruise were available at PANGAEA database (https://doi.org/10.1594/PANGAEA.971679; Avelina et al. 2024). To better understand the results and discussion, the cruises have been renamed according to the years of their respective austral summers (SUM; Table I).

Table I. List of oceanographic cruises carried out along the northern Antarctic Peninsula (NAP), summertime acronym, period of execution and number of oceanographic stations. The acronyms correspond to the southernmost Drake Passage (DP), the Bellingshausen Sea (BS), the Gerlache Strait (GS), the western (WB), central (CB), and eastern (EB) basins of Bransfield Strait and the western Weddell Sea (WS).

Oceanographic Cruise	Summertime Acronym	Period	Number of oceanographic stations per region						
			DP	BS	GS	WB	CB	EB	WS
FRUELA 95	SUM-95/96	December 1995	02	03	13	18	04	--	--
NAUTILUS I	SUM-14/15	February 2015	01	--	15	02	13	14	04
NAUTILUS II	SUM-15/16	February 2016	--	09	15	02	13	10	05
NAUTILUS III	SUM-16/17	February 2017	--	--	13	--	--	--	--
NAUTILUS IV	SUM-17/18	February 2018	--	--	15	--	--	--	--
NAUTILUS V	SUM-18/19	January 2019	--	--	15	--	--	--	--

The oceanographic cruises of NAUTILUS project were carried out on board the Brazilian Navy RV *NPo Almirante Maximiano*. The CTD-Rosette set from Sea Bird Electronics® Inc. (SBE) model SBE 911plus was used to measure the hydrographic parameters in the water column. The accuracy of the temperature and salinity sensors used corresponds to ± 0.001°C and ± 0.003, respectively (Dotto et al. 2021). Details of the FRUELA 1995 cruise and the acquisition of CTD hydrographic data are available in studies such as Doval et al. (2002) and García et al. (2002).

The upper mixed layer was estimated by a deviation in the potential density difference $\left(\frac{dp}{dz}\right)$, considering a variation of σ > 0.03 kg m^{-3} over a 10 m depth interval (de Boyer Montégut et al. 2004). The buoyancy or Brunt-Väisälä frequency (N in Hz) was determined by:

$$N = \sqrt{\left(\frac{g}{\rho}\right)\left(\frac{d\rho}{dz}\right)} \quad (1)$$

where g is gravity (m s^{-2}), ρ is the potential density (kg m^{-3}) of seawater and z is depth (m).

In order to assess the effects of freshwater input on the NAP, the percentage of meltwater (*MW*%) was estimated by:

$$MW\% = \left(1 - \frac{S_{surface} - 6}{S_{deep} - 6}\right) \times 100 \quad (2)$$

where $S_{surface}$ is the salinity of seawater measured at the surface and S_{deep} is the salinity at the deep layer. To calculate the MW% it was assumed that the average salinity value of sea ice is equal to 6 (Ackley et al. 1979). The above equation for estimating the percentage of meltwater has been widely used in the study region (e.g. Mendes et al. 2018, de Lima et al. 2019, Avelina et al. 2020, Costa et al. 2020).

Dissolved organic carbon

The sampling methods and analysis of DOC concentrations (μmol kg^{-1}) during the FRUELA 1995 cruise are available in Doval et al. (2002). All DOC sampling and analysis carried out during the NAUTILUS oceanographic cruises between 2015 and 2019 followed the same method described in da Cunha et al. (2018) and Avelina et al. (2020) for the Gerlache and Bransfield Straits, respectively. All the DOC samples from the NAUTILUS cruises were analyzed at the Marine Organic Geochemistry and Chemical Oceanography Laboratories of the Rio de Janeiro State University (Universidade do Estado do Rio de Janeiro – UERJ).

Briefly, during the FRUELA cruise all seawater samples for DOC analysis were filtered through 0.7 μm pore-sized filters (Doval et al. 2002). During the NAUTILUS cruises, while DOC samples collected at the surface mixed layer were also filtered (da Cunha et al. 2018), DOC samples collected below the mixed layer (depth > 100 m) were not filtered, since POC concentrations are low in deep water (Carlson et al. 2000, Dickson et al. 2007, da Cunha et al. 2018). Both FRUELA and NAUTILUS seawater samples for DOC analysis were kept frozen until they were analyzed in the respective laboratories.

The DOC samples were analyzed using a Shimadzu TOC L® Series analyzer, as non-purgeable organic carbon, in high-temperature catalytic combustion (Dickson et al. 2007). DOC samples were acidified and purged with scientific grade O_2 prior to analysis to ensure that all inorganic carbon was lost as CO_2 (Dickson et al. 2007, da Cunha et al. 2018). In addition, all samples were subjected to between three and five replicate injections (acceptable coefficient of variation < 1%). The carbon analyzers were standardized with solutions of potassium hydrogen phthalate (KHP) in Milli-Q® water.

The instrument blank was checked by measuring the DOC in Milli-Q® water with a low carbon content (DOC < 8 µmol kg^{-1}). While the accuracy of the FRUELA analysis system was tested in the international intercalibration exercise conducted by J. Sharp (University of Delaware; Doval et al. 2002), the accuracy of the NAUTILUS cruise analysis system was tested using a standard KHP solution (da Cunha et al. 2018). The excess DOC (ΔDOC) produced was calculated by subtracting the DOC concentrations at the surface and the average DOC concentration in deep water (44 µmol kg^{-1}; Romera-Castillo et al. 2016).

Estimation of the dissolved organic carbon diffusive fluxes

The diffusive fluxes of DOC ($F_{D\text{-}DOC}$ in mmol m^{-2} day^{-1}) were estimated using Fick's first law equation (Guo et al. 1995, Doval et al. 2002), considering the vertical gradient of DOC ($\frac{\Delta DOCz}{\Delta z}$) at the interval between two DOC samples collected:

$$F_{D\text{-}DOC} = -K_z \frac{\Delta DOCz}{\Delta z} \quad (3)$$

where K_z is the turbulent diffusion coefficient, which can be calculated from the equation:

$$K_z = \frac{\varepsilon}{N^2} \times \frac{R}{(1 - R)} \quad (4)$$

where the dissipation rate (ε) and the Richardson number (R) were set to constant values of 10^{-8} m^2 s^{-3} and 0.2, respectively, for the open sea (Doval et al. 2002).

To visualize the vertical fluxes, seven transects were defined along the NAP (see the map in the Figure 4). Positive $F_{D\text{-}DOC}$ values resulted from DOC concentrations that decreased with increasing depth, indicating net downward transport. The opposite process occurred when there was negative $F_{D\text{-}DOC}$ values, i.e. an increase in DOC concentrations with increasing depth, indicating upward net transport.

Circulation dynamics in the NAP and estimates of advective DOC fluxes

In order to understand the main ocean circulation patterns occurring in the NAP during the DOC sampling periods, we used monthly reanalysis data on zonal and meridional components of current velocity, obtained from GLORYS12V1, a product of the Copernicus Marine Environment Monitoring Service (https://doi.org/10.48670/moi-00021). The product was chosen due to the availability of data since 1993, covering the entire period studied. GLORYS12V1 has a horizontal resolution of 1/12° and 50 vertical levels. The model data was consistent with current velocity data measured in situ based on Acoustic Doppler Current Profiler (ADCP) along the Gerlache Strait (Su et al. 2022).

The average advective DOC flux ($\overline{F_{A\text{-}DOC}}$ in mol m^{-2} day^{-1}) in the first 250 m of the water column was estimated for each NAP region using the equation (Vetrov & Romankevich 2019):

$$\overline{F_{A\text{-}DOC}} = \overline{DOC} \times \left(\overline{u_0}^2 + \overline{v_0}^2\right)^{\frac{1}{2}} \quad (5)$$

where, $\overline{DOC}$ is the average DOC concentration (µmol kg^{-1}) and, $\overline{u_0}$ and $\overline{v_0}$ are, respectively, the average values of the zonal and meridional components of the current velocity (m s^{-1}).

Statistical analysis

Statistical analyses were carried out using the software JAMOVI© version 2.4.14 from 2023. The data was first tested for normality using the Shapiro-Wilk (W) statistical test, with a 95% confidence level.

The oceanographic variables, however, did not show a normal distribution (p-value < 0.05), making it necessary to use non-parametric statistics and the median as a measure of central tendency. To assess the differences between hydrographic conditions (i.e. temperature and salinity) between regions, the MANOVA test was used. The non-parametric Kruskal-Wallis test (H-test) was used to compare the median DOC concentrations in different regions of the NAP. The non-parametric Dwass-Steel-Critchlow-Fligner post hoc test (DSCF-test) was also applied to assess specific differences between regions.

RESULTS

Hydrographic conditions along the NAP

The NAP surface had the highest potential temperatures (θ > 1.0°C; Figure 2a) in Gerlache Strait and in the northern Bransfield Strait, between the central and eastern basins. Surface temperatures lower than 1.0°C were identified from the channel between the Drake Passage and the western basin of the Bransfield Strait, in the southwestern sector of the Bellingshausen Sea and in the southern Bransfield Strait, towards the Weddell Sea (Figure 2a). Surface salinities < 33.8 (Figure 2b) occurred mainly in the Bellingshausen Sea and Gerlache Strait, along with the highest MW% values. The western Bransfield Strait acted as a transition zone for the increase in surface salinity towards the central and eastern basins of the Bransfield Strait. However, the increase in salinity was interrupted by a core of low salinity near the Weddell Sea, associated with the increase in MW%.

The potential temperature-salinity diagram (Figures 2c, d) indicated that all regions of the NAP showed a signal from the intrusion and mixing of mCDW and DSW below 100 m depth. However, the greater volume of mCDW (θ > –0.5°C and salinity > 34.5; Ruiz Barlett et al. 2018) was observed in the southernmost Drake Passage, in the Bellingshausen Sea and at a maximum depth of 300 m, in the Gerlache Strait. DSW mainly occupied the intermediate and deep layers of the Gerlache and Bransfield Straits. It was also possible to identify the presence of HSSW (θ < –1.5°C and salinity >34.5; Dotto et al. 2016) at the bottom of the central basin of Bransfield Strait and LSSW (θ < –1.5°C and salinity < 34.5; Dotto et al. 2016) in the Weddell Sea, between 50 and 80 m. The statistical results confirmed that the NAP regions have different hydrographic conditions (MANOVA, p-value < 0.05).

DOC distribution along the NAP

DOC concentrations in the NAP ranged from 33.1 to 157.6 µmol kg^{-1}, with a median concentration of 48.7 µmol kg^{-1} (Table II). The western basin of Bransfield Strait had the highest median DOC concentration among the regions investigated, followed by the Gerlache Strait and the Bellingshausen Sea, all with median DOC concentrations > 50 µmol kg^{-1}. Median DOC concentrations < 50 µmol kg^{-1} occurred in the Drake Passage, the central and eastern basins of Bransfield Strait and the western Weddell Sea. In general, there were differences in DOC distributions between the regions of the NAP (Kruskal-Wallis, p-value < 0.05). The results of the DSCF-test statistical analyses are presented in Table III. The p-values < 0.05 indicate regional differences in DOC distribution.

At surface (Figure 3a), DOC accumulation occurred especially in the western Bransfield Strait and Gerlache Strait, producing an excess of DOC (ΔDOC) of 20 µmol kg^{-1}, compared to the DOC available in deep waters (~44 µmol kg^{-1}). High DOC concentrations (> 50 µmol kg^{-1}) could also be observed in the

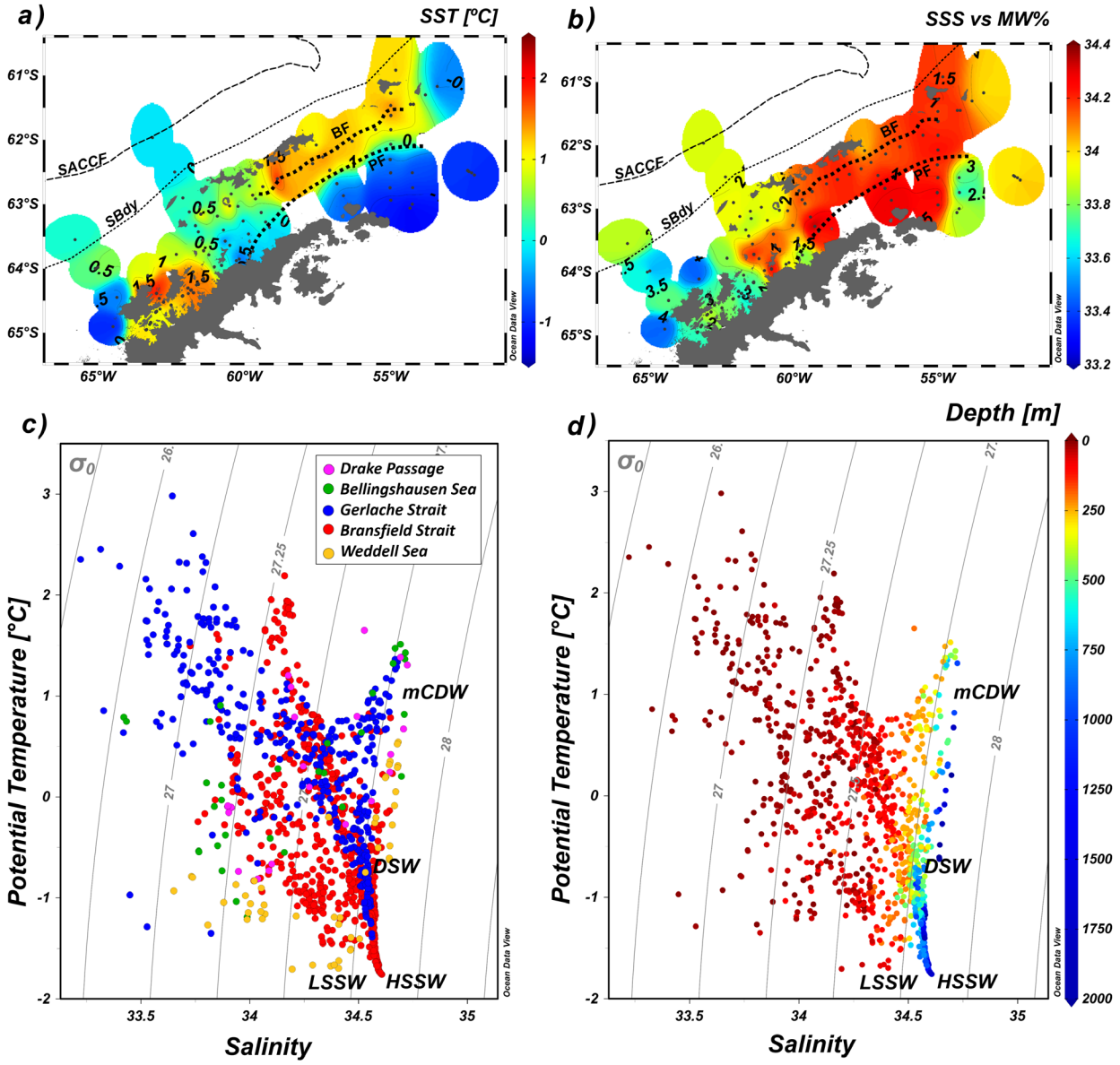

Figure 2. **Composites of a) sea surface temperature (SST in °C), b) sea surface salinity (SSS) versus meltwater percentage (MW%) along the northern Antarctic Peninsula; c) and d) Temperature-salinity diagram and water masses identification, where dots in c) indicate samples collected in the southernmost Drake Passage (magenta), the Bellingshausen Sea (green), the Gerlache (blue) and Bransfield Straits (red), and the Weddell Sea (yellow). Black lines in a) and b) correspond, respectively, to the Southern Antarctic Circumpolar Current Front (SACCF), the Southern Boundary of the ACC (SBdy), the Bransfield Front (BF) and Peninsula Front (PF). The color scale in d) corresponds to the depth of the water column (m). The acronyms correspond to modified Circumpolar Deep Water (mCDW), Dense Shelf Water (DSW), High-Salinity Shelf Water (HSSW) and Low-Salinity Shelf Water (LSSW).**

central Bransfield Strait and in the Bellingshausen Sea, especially near the coastal portions (Figure 3a). A peak of high DOC concentration, at the surface, also occurred at the point near the SACCF, in the southernmost Drake Passage (Figure 3a). Low DOC concentrations (< 45 µmol kg^{-1}) were observed mainly at the surface of the eastern Bransfield Strait. However, DOC concentrations increased again towards the Weddell Sea (ΔDOC ~15 µmol kg^{-1}; Figure 3a).

Table II. Regions of the northern Antarctic Peninsula, cruise period, n-samples and the minimum, maximum and median concentrations of dissolved organic carbon (DOC in µmol kg^{-1}).

Region	Period	N-samples	Minimum	Maximum	Median
Southernmost Drake Passage	SUM-95/96	14	38.9	112.0	55.0
	SUM-14/15	9	38.1	64.0	47.1
	Total	23	38.1	112.0	49.6
Bellingshausen Sea	SUM-95/96	17	40.9	126.6	58.4
	SUM-15/16	23	36.8	62.3	44.9
	Total	40	36.8	126.6	50.7
Gerlache Strait	SUM-95/96	46	36.0	155.8	54.5
	SUM-14/15	88	43.5	84.0	48.9
	SUM-15/16	106	35.3	116.1	50.2
	SUM-16/17	75	41.9	157.6	78.1
	SUM-17/18	82	43.2	90.0	50.7
	SUM-18/19	35	35.1	81.4	52.2
	Total	432	35.1	157.6	51.6
Western Bransfield Strait	SUM-95/96	110	36.0	131.4	57.9
	SUM-14/15	14	46.5	65.5	52.3
	SUM-15/16	13	39.4	54.4	44.0
	Total	137	36.0	131.4	54.4
Central Bransfield Strait	SUM-95/96	23	38.9	77.9	54.5
	SUM-14/15	97	39.0	88.4	47.3
	SUM-15/16	97	33.3	106.1	45.0
	Total	217	33.3	106.1	46.2
Eastern Bransfield Strait	SUM-14/15	104	37.9	115.8	46.6
	SUM-15/16	82	33.1	90.5	42.6
	Total	186	33.1	115.8	44.7
Western Weddell Sea	SUM-14/15	34	38.6	88.4	44.0
	SUM-15/16	26	33.3	66.1	48.4
	Total	60	33.3	88.4	44.5
NAP	Total	1095	33.1	157.6	48.7

DOC concentrations between 33 and 45 µmol kg^{-1} occurred throughout the NAP water column (Figure 3b). DOC concentrations > 45 µmol kg^{-1} were dominant from the surface up to ~2000 m depth (Figure 3b). The western sector of the NAP (longitudes > 60°W) had the highest DOC concentrations (> 75 µmol kg^{-1}) above 800 m (Figure 3b). Considering depths > 250 m, DOC concentrations were generally higher in the mCDW (~51 µmol kg^{-1}) than the DSW (~47.5 µmol kg^{-1}; Figure 3c).

Diffusive fluxes of DOC along the NAP

The $F_{D\text{-}DOC}$ results in the NAP water column ranged from –624.1 to 1629.9 mmol m^{-2} day^{-1}, with a median $F_{D\text{-}DOC}$ of 0.24 mmol m^{-2} day^{-1}. In the upper 250 m of the NAP water column (i.e. the depth interval with the largest *n*-sample and highest median DOC concentration) the median value of net downward DOC transport increased slightly to 0.30 mmol m^{-2} day^{-1}. The intermediate layer (250 m < depth ≤ 750 m) and the deep layer (depth > 750m) of the NAP had an upward net transport of DOC, with median $F_{D\text{-}DOC}$ of –0.17 and –0.37 mmol m^{-2} day^{-1}, respectively.

The regional analysis of the first 250 m of the water column showed that the southernmost Drake Passage had the highest median value for the net downward transport of DOC (1.70 mmol m^{-2} day^{-1}), followed by the Bellingshausen Sea (0.60 mmol m^{-2} day^{-1}) and the Bransfield Strait (0.38 mmol m^{-2} day^{-1}). The Gerlache Strait had the lowest median value for net downward DOC transport (0.24 mmol m^{-2} day^{-1}). The Weddell Sea was the only region of the NAP that showed an upward net transport of DOC in the first 250 m of the water column (–0.37 mmol m^{-2} day^{-1}). However, there were no regional differences between DOC diffusive fluxes (Kruskal-Wallis, *p*-value ≥ 0.05).

The vertical profiles of $F_{D\text{-}DOC}$, in the upper 250 m (Figure 4), showed that the greatest downward and/or upward diffusive fluxes of DOC occurred near the NAP ocean fronts (0°C isotherm). The highest downward DOC fluxes ($F_{D\text{-}DOC}$, > 10 mmol m^{-2} day^{-1}) were associated with the front near Anvers Island (Figure 4a), the SACCF and the Antarctic Peninsula (Figure 4b) and Snow Island (Figure 4c). On the other hand, SBdy (Figures 4a, b) was associated with upward DOC fluxes ($F_{D\text{-}DOC}$ < –10 m^{-2} day^{-1}). Along the transects located in the central (Figure 4f) and eastern basins of Bransfield Strait (Figure 4g), where the Peninsula and Bransfield Fronts are well established, the high downward DOC fluxes were positioned to the north of the Peninsula Front, while the high upward DOC fluxes were to the south of the Peninsula Front.

Table III. *p*-values for the Dwass-Steel-Critchlow-Fligner statistical test for regional dissolved organic carbon distribution.

	Southernmost Drake Passage	Bellingshausen Sea	Gerlache Strait	Western Bransfield Strait	Central Bransfield Strait	Eastern Bransfield Strait
Bellingshausen Sea	1.000	-	-	-	-	-
Gerlache Strait	0.898	0.725	-	-	-	-
Western Bransfield Strait	0.731	0.481	0.910	-	-	-
Central Bransfield Strait	0.329	0.125	< 0.001*	< 0.001*	-	-
Eastern Bransfield Strait	0.036*	0.006*	< 0.001*	< 0.001*	0.200	-
Western Weddell Sea	0.399	0.181	< 0.001*	< 0.001*	0.977	0.999

Note: (*) Differences in DOC distributions between the regions of the northern Antarctic Peninsula (*p*-value < 0.05).

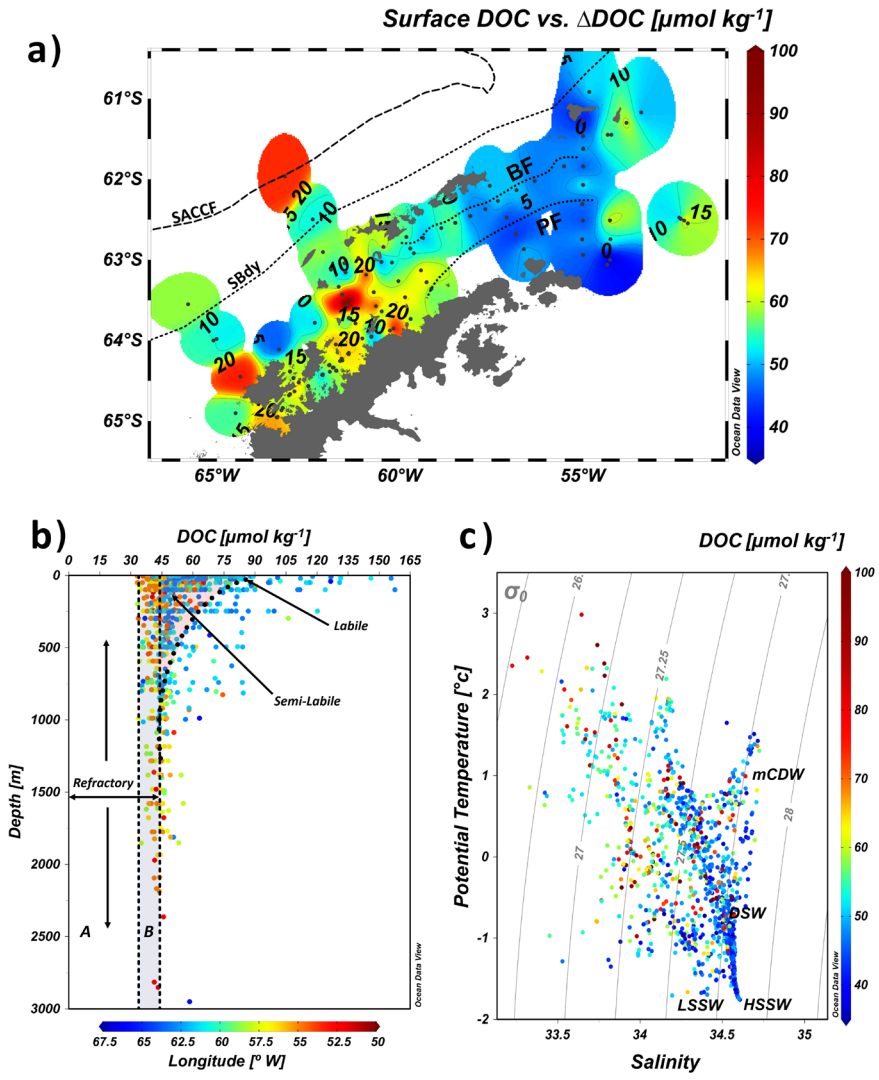

Figure 3. a) Composite distribution of dissolved organic carbon (DOC in µmol kg^{-1}) at the sea surface versus excess DOC (ΔDOC in µmol kg^{-1}) produced in the northern Antarctic Peninsula. Black lines correspond, respectively, to the Southern Antarctic Circumpolar Current Front (SACCF), the Southern Boundary of the ACC (SBdy), the Bransfield Front (BF) and Peninsula Front (PF). b) Vertical distribution of dissolved organic carbon (DOC in µmol kg^{-1}) with the DOC ocean reservoir conceptual model (Carlson 2002). The refractory reservoir is divided according to the DOC cycling time in the water column: (A) millennia and (B) centuries. c) Temperature-salinity diagram as a function of DOC concentrations and identification of water masses in the north of the Antarctic Peninsula. The acronyms correspond to modified Circumpolar Deep Water (mCDW). Deep Shelf Water (DSW). High-Salinity Shelf Water (HSSW) and Low-Salinity Shelf Water (LSSW).

NAP circulation dynamics and estimates of DOC advective fluxes

During the study period, the NAP had the highest average geostrophic velocities (> 0.2 m s^{-1}) in the southernmost Drake Passage, between SACCF and SBdy, while the lowest velocities (< 0.15 m s^{-1}) occurred mainly in the western Weddell Sea (Figure 5a). In this ocean circulation scenario, the NAP had a mean advective flux of DOC of 276.3 mol m^{-2} day^{-1} in the upper 250 m (Figure 5b). In this depth range (Figure 5b), the southernmost Drake Passage had the highest average horizontal DOC transport of 515.1 mol m^{-2} day^{-1}, followed by the Bellingshausen Sea with 275.5 mol m^{-2} day^{-1}, the Bransfield Strait with 191.5 mol m^{-2} day^{-1} and Gerlache Strait with 128.2 mol m^{-2} day^{-1}. The lowest average advective flux of DOC of 75.2 mol m^{-2} day^{-1} occurred in the Weddell Sea (Figure 5b).

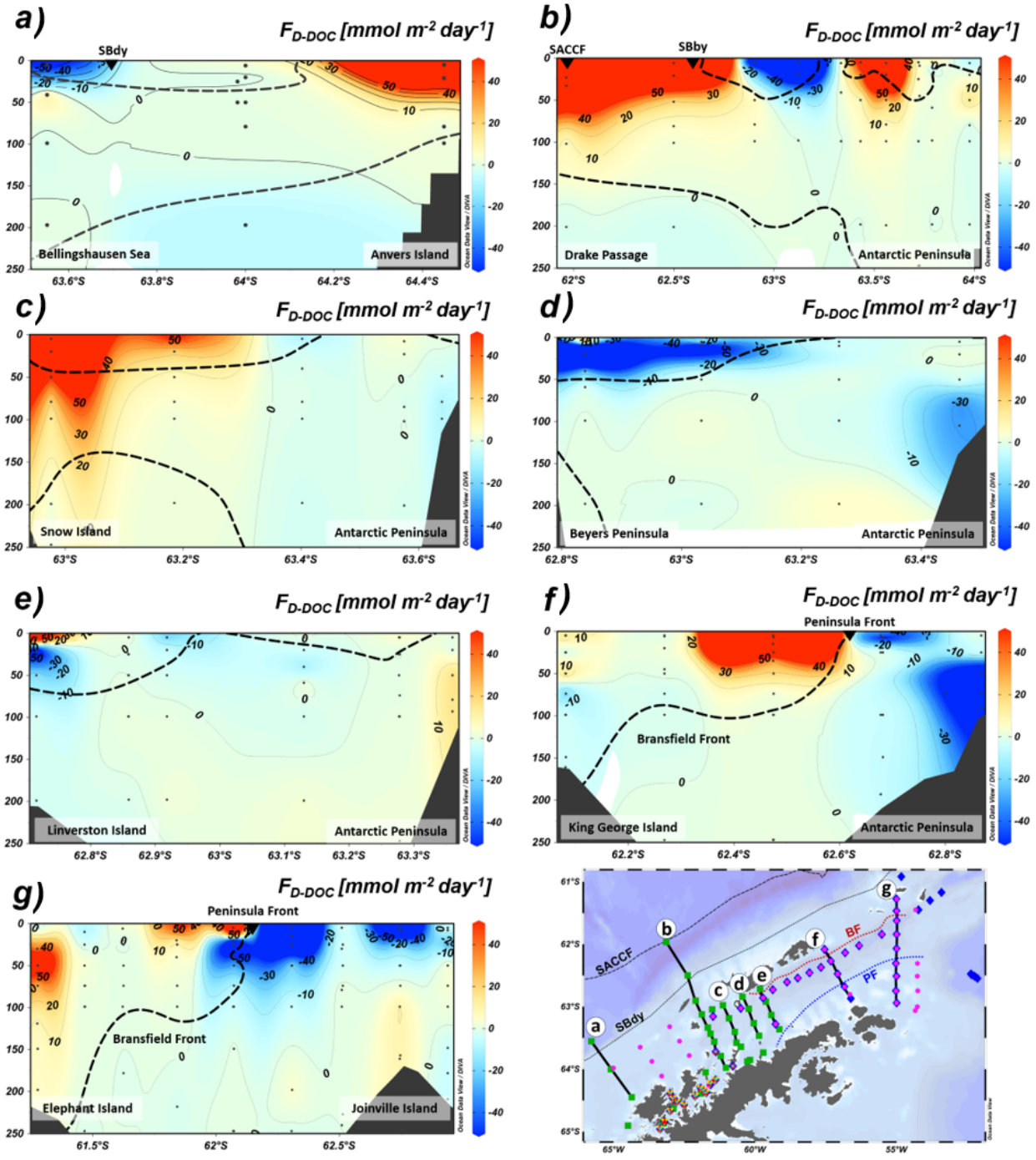

Figure 4. a-g) Vertical diffusive fluxes of dissolved organic carbon ($F_{D\text{-}DOC}$ in mmol m^{-2} day^{-1}) across the northern Antarctic Peninsula. The thin black isolines in panels a) to g) indicate the $F_{D\text{-}DOC}$ between –50 and 50 mmol m^{-2} day^{-1} at each interval of 10 mmol m^{-2} day^{-1}. The thick black dashed lines in panels a) to g) mark the position of the 0°C isotherm. The letters a to g in the bottom right panel indicate the positions of the sections corresponding to panels a) to g), respectively. The dashed and dotted lines on the map correspond, respectively, to the Southern Antarctic Circumpolar Current Front (SACCF), the Southern Boundary of the ACC (SBdy), the Bransfield Front (BF) and Peninsula Front (PF).

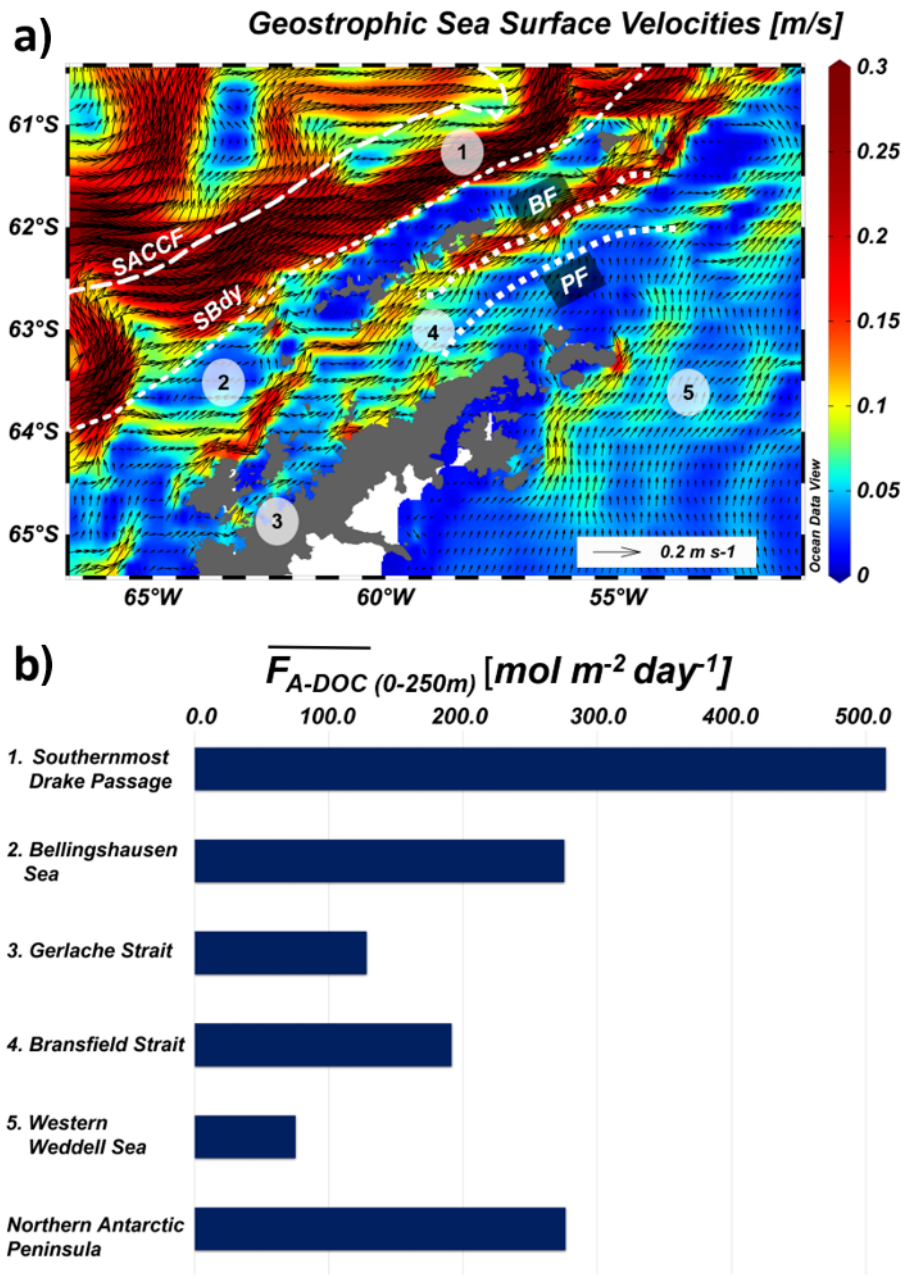

Figure 5. a) Map of average geostrophic sea surface velocities (m s^{-1}) between 1995 and 2015-2019, along the northern Antarctic Peninsula (NAP) based on GLORYS12V1. The vectors correspond to the intensity and direction of the surface current. The white lines correspond, respectively, to the Southern Antarctic Circumpolar Current Front (SACCF), the Southern Boundary of the ACC (SBdy), the Bransfield Front (BF) and Peninsula Front (PF). The numbers (1-5) indicate the subregions of the NAP. b) Bar graph for the average advective fluxes of dissolved organic carbon (F_{A-DOC} in mol m^{-2} day^{-1}) in the upper 250 m.

DISCUSSION

Regional aspects controlling the distribution of DOC along the NAP

The DOC concentrations presented here (33.1 – 157.6 µmol kg^{-1}) were within the concentration range commonly found in other sectors of the Southern Ocean, which is between 33 µmol kg^{-1} and 195 µmol kg^{-1} (e.g. Wiebinga & De Baar 1998, Ogawa et al. 1999, Bercovici & Hansell 2016, Bercovici et al. 2017, Fang et al. 2020, 2023). Three main factors can be considered responsible for the distribution and control of DOC throughout the water column: (i) the intensity of biological activity in the upper mixed layer, responsible for the formation of organic matter (Ducklow et al. 1995, 2007, Doval et al. 2002,

Costa et al. 2020); (ii) the vertical stratification of the water column, which is important for allowing DOC to accumulate in the upper mixed layer during primary production (da Cunha et al. 2018, Avelina et al. 2020) and; (iii) the vertical export and degradation of organic matter, which is important in the processes of transport and removal of DOC throughout the water column (Bercovici & Hansell 2016, Bercovici et al. 2017, Fang et al. 2020).

We observed significant regional differences along the NAP environment in both its hydrographic conditions and DOC distribution over the 6 years of observations, which reflects the high interannual variability and the patch distribution of physical and biogeochemical provinces along the study area (Testa et al. 2021). Previous studies carried out in the NAP (e.g. Doval et al. 2002, da Cunha et al. 2018, Avelina et al. 2020, Jang et al. 2020) evaluated the spatial and/or temporal variability of DOC only in the Gerlache and Bransfield Straits, without considering other regions around the NAP. Moreover, Testa et al. (2021) evaluated the physical and biogeochemical regionalization of the Southern Ocean; however, without considering the distribution of DOC. Thus, this study advances in presenting an integrated evaluation of this complex environmental system using DOC as a biogeochemical proxy.

The multiple comparisons test showed that there are three systems governing the distribution of DOC in the NAP. The first system connected the distribution of DOC between the southernmost Drake Passage, the Bellingshausen Sea, the Gerlache Strait and the western basin of Bransfield Strait. The regional coupling was characterized by the highest DOC concentrations in the NAP (median 52.03 $\mu mol\ kg^{-1}$) as well as DOC concentrations that deviated from the conceptual model of DOC reservoir for the open ocean (DOC > 80 $\mu mol\ kg^{-1}$; Figure 3b; Carlson 2002). High DOC concentrations may be a result of phytoplankton production, POC solubilization and particle export due to melting sea ice (Doval et al. 2002, da Cunha et al. 2018, Fang et al. 2023).

In the southernmost Drake Passage, the SACCF and its meanders and eddies may have produced an excess of DOC through the formation of phytoplankton biomass (Kahru et al. 2007) and zooplankton (Ward et al. 2002). The Bellingshausen Sea, the Gerlache Strait and the western Bransfield Strait are the shallowest and geographically closest areas of the NAP. The high production of DOC in these three sectors may reflect the biological activity in the euphotic zone and the stratification of the water column due to the presence of the mCDW (Mendes et al. 2012, 2018, Costa et al. 2023). Doval et al. (2002) considered that the excess of DOC produced in a shallow mixed layer in the Gerlache Strait and the western basin of the Bransfield Strait, during SUM-95/96, was probably of phytogenic origin. Furthermore, the DOC was the main contributor to the export of organic matter (Doval et al. 2002). da Cunha et al. (2018) described that the DOC accumulation in the surface layer of the water column of the Gerlache Strait in SUM-14/15 and SUM-15/16 was related to higher net community production and higher nitrate deficit due to primary production (Romera-Castillo et al. 2016, Monteiro et al. 2023). In SUM-15/16 there was also a large diatoms bloom (Costa et al. 2020, 2021), associated with a El Niño and a greater influx of cold waters from the Weddell Sea (Costa et al. 2021). Moreover, the mCDW, from the Bellingshausen Sea, was present in the western basin of the Bransfield Strait, increasing DOC concentrations in SUM-15/16 (Avelina et al. 2020).

The input of meltwater from the Antarctic Peninsula and the surrounding islands can also affect surface DOC production. During SUM-16/17, the Gerlache Strait had the highest median DOC concentration (78 $\mu mol\ kg^{-1}$). For this same period, Lopez & Hansell (2023) identified that, in the Pacific sector of the Southern Ocean, the high melting of sea ice enriched surface waters with iron, boosting

the export of particles and the release of DOC into the deep ocean. Thus, the coastal conditions and restricted circulation of the Gerlache Strait (García et al. 2002, Zhou et al. 2002, da Cunha et al. 2018), associated with the melting of ice in the Southern Ocean, caused by the El Niño of record intensity, which occurred throughout 2016 (Vera & Osman 2018), may have caused an unprecedented export of particles and DOC. Moreover, the rebalancing of climate mode conditions may have favored the decrease in DOC concentrations observed in SUM-17/18 and SUM-18/19.

The second system of DOC distribution connected the southernmost Drake Passage and the Bellingshausen Sea with the central basin of the Bransfield Strait and the Weddell Sea. The relatively lower DOC concentrations of 47 μmol kg^{-1} throughout the water column (Carlson 2002, Avelina et al. 2020) seems to be mainly responsible for the apparent similarity in DOC distribution between Bellingshausen-Drake with the central basin of the Bransfield Strait and the Weddell Sea. As occurs in the western sector of the NAP, sea ice also increases DOC concentrations along the Weddell Sea, via particle sinking (Fang et al. 2023). However, microorganisms remineralize part of the exported organic matter, decreasing DOC concentrations throughout the water column (Signori et al. 2014, 2018, Avelina et al. 2020, Cai & Jiao 2023).

The differences in DOC distributions were also interesting because it confirms the decoupling between the DOC distributions of the western and central basins of Bransfield Strait. This dynamic indicates that while the western basin of Bransfield Strait produces excess DOC at the surface, the central basin seems to be mostly dominated by the processes of decomposition of organic matter (Avelina et al. 2020), associated with increased levels of CO_2 (Santos-Andrade et al. 2023) and dissolved inorganic nutrients (Monteiro et al. 2023) towards the bottom. Parameters such as phytoplankton biomass and POC also indicated a pattern of decoupling between the western and central basins of Bransfield Strait (Testa et al. 2021).

Besides regional differences, interannual variability in DOC distribution is also an important factor along the Bransfield Strait. For instance, Avelina et al. (2020) showed that the significant differences between DOC concentrations and other physicochemical parameters of seawater in the Bransfield Strait between SUM-14/15 and SUM -15/16 were related to changes in the structure of the water column caused by the combined action of ENSO and SAM. During SUM-14/15, the NAP had greater intrusions of mCDW, in both El Niño and positive SAM of weak intensity. On the other hand, in SUM-15/16 there were greater contributions of DSW (Avelina et al. 2020), favoring even the intrusion of HSSW along the deep basin of Bransfield Strait (Dotto et al. 2016, Damini et al. 2022).

The third system of DOC distribution connected in the deep layers (> 800 m) the western Weddell Sea with the eastern and central basins of Bransfield Strait (east to west direction). The coupling showed a median DOC concentration of 45.5 μmol kg^{-1}. Despite the occasional enrichment of DOC via particle sinking (Fang et al. 2023, Lopez & Hansell 2023), below 400 m DOC concentrations along the NAP generally show constant distribution (~44 μmol kg^{-1}) and are typical of recalcitrant organic carbon (Doval et al. 2002, Bercovici & Hansell 2016, Avelina et al. 2020, Fang et al. 2020).

Overall, our results indicate that there are three patterns of DOC distribution along the NAP. The shallower regions of the southernmost Drake Passage, Bellingshausen Sea, Gerlache Strait and western Bransfield Strait, were the areas with the highest DOC production and probably high DOC export to deep layers. The intermediate waters of the southernmost Drake Passage, the Bellingshausen Sea, the central Bransfield Strait and the western Weddell Sea have relatively lower DOC concentrations

than surface waters, with probable dominance of organic matter degradation. Finally, the deep waters of the western Weddell Sea, eastern and central Bransfield, have the lowest DOC concentrations of the NAP with a probable dominance of recalcitrant DOC.

The oceanographic particularities of each NAP region and the variability in DOC distributions reflect the influence of the flows of the Antarctic Circumpolar Current and the Weddell Gyre in the ocean regions of the NAP (Dotto et al. 2016, Kerr et al. 2018a, Ruiz Barlett et al. 2018, Dotto et al. 2021, Damini et al. 2022) as well as the occurrence of meltwater near coastal regions (Loeb et al. 2010, da Cunha et al. 2018, Monteiro et al. 2020, Lopez & Hansell 2023). Our regionalization of NAP from DOC distribution corroborated the results described by Testa et al. (2021) for different biogeochemical parameters on the effects of sea ice cover and water column depth.

Importance of vertical and horizontal fluxes for DOC exports at the NAP

The median value of diffusive fluxes DOC ($F_{D\text{-}DOC}$ = 0.24 mmol m^{-2} day^{-1}) showed that there is a net downward transport trend along the NAP. The results of this study confirmed that the NAP kept the $F_{D\text{-}DOC}$ values extremely low, as observed by Doval et al. (2002) along the Gerlache Strait and the western basin of Bransfield Strait during SUM-95/96. Lovecchio et al. (2023) showed that the diffusive fluxes of DOC corresponded to < 0.1% of the total organic carbon exported near South Georgia Island. The $F_{D\text{-}DOC}$ median values observed in the NAP were also close to those observed by Guo et al. (1995) in the Gulf of Mexico (0.36 mmol m^{-2} day^{-1}) and in the Mid-Atlantic Bight (0.18 mmol m^{-2} day^{-1}).

Guo et al. (1995), Doval et al. (2002) and Lovecchio et al. (2023) justified their findings considering that POC plays an important role in the vertical export of DOC. They also considered that advective fluxes were probably the main export pathway for DOC; however, they did not quantify horizontal transport. Therefore, our study confirmed that the NAP average advective flux of DOC (276.3 mol m^{-2} day^{-1}) is 10^6 times higher than the diffusive fluxes of DOC. Our results also suggest that the average of horizontal fluxes of DOC along the NAP, in the first 250 m of depth, correspond to between 5% and 35% of the maximum advective flux of DOC observed in the Arctic Ocean (Vetrov & Romankevich 2019). The horizontal transport patterns of DOC are important for understanding the supply of chemical energy to areas with low DOC production (Santinelli et al. 2021).

Despite the low net downward transport trend, our results also indicate that the ocean fronts of the NAP play a fundamental role in increasing diffusive fluxes of DOC. The SACCF (Orsi et al. 1995), in the southernmost Drake Passage, the Peninsula Front, in the Bransfield Strait (García et al. 2002, Sangrà et al. 2011), and the gradients formed by the input of meltwater, were responsible for producing downward DOC fluxes > 50 mmol m^{-2} day^{-1}. These values exceed the maximum value of net downward DOC transport observed in the Peruvian upwelling system in the South Pacific ($F_{D\text{-}DOC}$ = 31 mmol m^{-2} day^{-1}; Loginova et al. 2018). The influx of cold water along the shelf of the NAP was in turn responsible for inducing an upward flux of DOC. The flow of DSW through the Weddell Sea produced an upward flux of DOC of –0.37 mmol m^{-2} day^{-1}. The SBdy (Orsi et al. 1995) and the southern sector of the Peninsula Front produced the highest upward diffusive fluxes of DOC < –50 mmol m^{-2} day^{-1}. Therefore, in the same way that ocean fronts are important for the physical-biological coupling (Chapman et al. 2020), these mesoscales structures also play a fundamental role in the biogeochemical cycles of DOC.

CONCLUSIONS

We investigate the regional aspects controlling the distribution and diffusive and advective fluxes of DOC along the southernmost Drake Passage, Bellingshausen Sea, Gerlache and Bransfield Straits and Weddell Sea, during distinct austral late summer conditions. Thus, presenting a novel integrated assessment of the DOC distribution and vertical/advective fluxes along the NAP environments. The greater coverage of the sampling points along the NAP and the continuity of annual monitoring have made it possible to present an overview of the distribution of DOC and the main physical and biogeochemical aspects prevailing in each subregion. The NAP had significant regional differences in both its hydrographic conditions and DOC distribution. The regional variability reflected the main biogeochemical sources and fates of DOC throughout the water column, such as phytoplankton production, particle export and microbial degradation associated with the Antarctic Circumpolar Current inflows, the Weddell Gyre transport and the meltwater input. DOC diffusive fluxes along the NAP were extremely low, confirming that DOC export depends on particle fluxes to the deep ocean. However, the various ocean fronts present in the NAP proved to be key areas for observations of downward and upward DOC fluxes. In addition, advective flux was an efficient mechanism to transport DOC along the NAP. These results show that DOC can be used as an important proxy for evaluating the coupling between physical, biogeochemical and climate processes over time.

Acknowledgments

The authors would like to thank M. L. C. Ferreira, R. A. Keim, H. Soares (*in memoriam*) and L. Amorim for help with sampling and DOC analysis. The authors also thank the Brazilian Navy, especially the officers and crew, and all the researchers onboard of the RV NPo. *Almirante Maximiano*, for providing logistical and sampling support during the NAUTILUS cruises. GOAL has been supported from the Conselho Nacional de Desenvolvimento Científico e Tecnológico (CNPq Grant Nos. 405869/2013-4, 407889/2013-2, 442628/2018-8, 442637/2018-7, 440865/2023-9, and 440859/2023-9), the Coordenação de Aperfeiçoamento de Pessoal de Nível Superior – Brasil (CAPES Grant No. 23038.001421/2014-30) and Instituto Nacional de Ciência e Tecnologia da Criosfera (INCT-CRIOSFERA; CNPq Grant Nos. 573720/2008-8 and 465680/2014-3; FAPERGS Grant No. 17/2551-0000518-0). This study was financed in part by CAPES – Finance Code 001. R.A acknowledges CAPES PhD Grant No. 88887.486629/2020-00 and CNPq Grant Nos. 200260/2022-7 and 401820/2022-0. L.C.C acknowledges CNPq Grant No. 309708/2021-4, FAPERJ (Fundação de Amparo à Pesquisa do Estado do Rio de Janeiro) Grant No. E-26/201.156/2022, and Prociência/UERJ grant 2021-2024. R.K and M.M.M acknowledge CNPq Grants No. 309978/2021-1 and 309653/2021-5, respectively.

REFERENCES

ACKLEY SF, BUCKT KR & TAGUCHI S. 1979. Standing crop of algae in the sea ice of the Weddell Sea region. Deep Sea Res 26: 269-281.

ANADÓN R & ESTRADA M. 2002. The FRUELA cruises. Deep Sea Res 2 Top Stud Oceanogr 49: 567-583.

AVELINA R, DA CUNHA LC, FARIAS C DE O, HAMACHER C, KERR R & MATA MM. 2020. Contrasting dissolved organic carbon concentrations in the Bransfield Strait, Northern Antarctic Peninsula: insights into ENSO and SAM effects. J Mar Syst 212: 103457.

AVELINA R, DA CUNHA LC, KERR R, FARIAS C DE O, HAMACHER C & MATA MM. 2024. Dissolved organic carbon along the northern Antarctic Peninsula during Almirante Maximiano cruises NAUTILUS (2015-2019). PANGAEA. Available at: https://doi.org/10.1594/PANGAEA.971679.

BERCOVICI SK & HANSELL DA. 2016. Dissolved organic carbon in the deep Southern Ocean: Local versus distant controls. Global Biogeochem Cycles 30: 350-360.

BERCOVICI SK, HUBER BA, DEJONG HB, DUNBAR RB & HANSELL DA. 2017. Dissolved organic carbon in the Ross Sea: Deep enrichment and export. Limnol Oceanogr 62: 2593-2603.

CAI R & JIAO N. 2023. Recalcitrant dissolved organic matter and its major production and removal processes in the ocean. Deep Sea Res 1 Oceanogr Res Pap 191: 103922.

CARLSON CA. 2002. Production and Removal Processes. In: Biogeochemistry of Marine Dissolved Organic Matter, Elsevier, p. 91-151.

CARLSON CA, HANSELL DA, PELTZER ET & SMITH WO. 2000. Stocks and dynamics of dissolved and particulate organic matter in the southern Ross Sea, Antarctica. Deep Sea Res 2 Top Stud Oceanogr 47: 3201-3225.

CHAPMAN CC, LEA MA, MEYER A, SALLÉE JB & HINDELL M. 2020. Defining Southern Ocean fronts and their influence on biological and physical processes in a changing climate. Nat Clim Chang 10: 209-219.

COSTA RR, FERREIRA A, DE SOUZA MS, TAVANO VM, KERR R, SECCHI ER, BROTAS V, DOTTO TS, BRITO AC & MENDES CRB. 2023. Physical-biological drivers modulating phytoplankton seasonal succession along the Northern Antarctic Peninsula. Environ Res 231: 116273.

COSTA RR, MENDES CRB, FERREIRA A, TAVANO VM, DOTTO TS & SECCHI ER. 2021. Large diatom bloom off the Antarctic Peninsula during cool conditions associated with the 2015/2016 El Niño. Commun Earth Environ 2: 252.

COSTA RR, MENDES CRB, TAVANO VM, DOTTO TS, KERR R, MONTEIRO T, ODEBRECHT C & SECCHI ER. 2020. Dynamics of an intense diatom bloom in the Northern Antarctic Peninsula, February 2016. Limnol Oceanogr 65: 2056-2075.

DA CUNHA LC, HAMACHER C, FARIAS C DE O, KERR R, MENDES CRB & MATA MM. 2018. Contrasting end-summer distribution of organic carbon along the Gerlache Strait, Northern Antarctic Peninsula: Bio-physical interactions. Deep Sea Res 2 Top Stud Oceanogr 149: 206-217.

DAMINI BY, KERR R, DOTTO TS & MATA MM. 2022. Long-term changes on the Bransfield Strait deep water masses: Variability, drivers and connections with the northwestern Weddell Sea. Deep Sea Res 1 Oceanogr Res Pap 179: 103667.

DE BOYER MONTÉGUT C, MADEC G, FISCHER AS, LAZAR A & IUDICONE D. 2004. Mixed layer depth over the global ocean: An examination of profile data and a profile-based climatology. J Geophys Res Oceans 109: 1-20.

DE LIMA DT, MOSER GAO, PIEDRAS FR, DA CUNHA LC, TENENBAUM DR, TENÓRIO MMB, DE CAMPOS MVPB, CORNEJO T DE O & BARRERA-ALBA JJ. 2019. Abiotic changes driving microphytoplankton functional diversity in Admiralty bay, King George island (Antarctica). Front Mar Sci 6: 1-17.

DICKSON AG, SABINE CL & CHRISTIAN JR. 2007. Guide to best practices for ocean CO_2 measurements. North Pacific Marine Science Organization, 191 p.

DOTTO TS, KERR R, MATA MM & GARCIA CAE. 2016. Multidecadal freshening and lightening in the deep waters of the Bransfield Strait, Antarctica. J Geophys Res Oceans 121: 3741-3756.

DOTTO TS, MATA MM, KERR R & GARCIA CAE. 2021. A novel hydrographic gridded data set for the northern Antarctic Peninsula. Earth Syst Sci Data 13: 671-696.

DOVAL D, ÁLVAREZ-SALGADO XA, CASTRO CG & PÉREZ FF. 2002. Dissolved organic carbon distributions in the Bransfield and Gerlache Straits, Antarctica. Deep Sea Res 2 Top Stud Oceanogr 49: 663-674.

DUCKLOW H, STEINBERG D & BUESSELER K. 2001. Upper Ocean Carbon Export and the Biological Pump. Oceanography 14: 50-58.

DUCKLOW HW, BAKER K, MARTINSON DG, QUETIN LB, ROSS RM, SMITH RC, STAMMERJOHN SE, VERNET M & FRASER W. 2007. Marine pelagic ecosystems: The West Antarctic Peninsula. Philos Trans R Soc Lond B: Biol Sci 362: 67-94.

DUCKLOW HW, CARLSON CA, BATES NR, KNAP AH, MICHAELS AF, JICKELLS T, PJB WILLIAMS & IN MCCAVE. 1995. Dissolved organic carbon as a component of the biological pump in the North Atlantic Ocean. Philos Trans R Soc Lond B Biol Sci 348: 161-167.

FABRÉS J, CALAFAT A, CANALS M, BÁRCENA MA & FLORES JA. 2000. Bransfield Basin fine-grained sediments: late-Holocene sedimentary processes and Antarctic oceanographic conditions. Holocene 10: 703-718.

FANG L, LEE SH, LEE SA, HAHM D, KIM G, DRUFFEL ERM & HWANG J. 2020. Removal of Refractory Dissolved Organic Carbon in the Amundsen Sea, Antarctica. Sci Rep 10: 1213.

FANG Z, ZHANG K, YANG W, CHEN M, STUBBINS A & HU H. 2023. Top-down control over dissolved organic carbon in the bottom water of the Weddell Sea and its implication for the continental shelf pump. Prog Oceanogr 219: 103145.

FRIEDLINGSTEIN P ET AL. 2019. Global carbon budget 2019. Earth Syst Sci Data 11: 1783-1838.

FRIEDLINGSTEIN P ET AL. 2023. Global Carbon Budget 2023. Earth Syst Sci Data 15: 5301-5369.

GARCÍA MA, CASTRO CG, RÍOS AF, DOVAL MD, ROSÓN G, GOMIS D & LÓPEZ O. 2002. Water masses and distribution of physico-chemical properties in the Western Bransfield Strait and Gerlache Strait during Austral summer 1995/96. Deep Sea Res 2 Top Stud Oceanogr 49: 585-602.

GUO L, SANTSCHI PH & WARNKEN KW. 1995. Dynamics of dissolved organic carbon (DOC) in oceanic environments. Limnol Oceanogr 40: 1392-1403.

HANSELL DA & CARLSON CA. 1998a. Deep-ocean gradients in the concentration of dissolved organic carbon. Nature 395: 263-266.

HANSELL DA & CARLSON CA. 1998b. Net community production in dissolved organic carbon. Global Biogeochem Cycles 12: 443-453.

HANSELL DA, CARLSON CA, AMON RMW, ANTÓN ÁLVAREZ-SALGADO X, YAMASHITA Y, ROMERA-CASTILLO C, BIF MB & KOZYR A. 2021. Compilation of dissolved organic matter (DOM) data obtained from global ocean observations from 1994 to 2020 (NCEI Accession 0227166). NOAA National Centers for Environmental Information.

HANSELL DA, CARLSON CA & SUZUKI Y. 2002. Dissolved organic carbon export with North Pacific Intermediate Water formation. Global Biogeochem Cycles 16: 1-8.

HANSELL D, CARLSON C, REPETA D & SCHLITZER R. 2009. Dissolved Organic Matter in the Ocean: A Controversy Stimulates New Insights. Oceanography 22: 202-211.

HENLEY SF ET AL. 2020. Changing Biogeochemistry of the Southern Ocean and Its Ecosystem Implications. Front Mar Sci 7: 581.

HUNEKE WGC, HUHN O & SCHRÖEDER M. 2016. Water masses in the Bransfield Strait and adjacent seas, austral summer 2013. Polar Biol 39: 789-798.

JANG J, PARK J, AHN S, PARK KT, HA SY, PARK J & CHO KH. 2020. Molecular-Level Chemical Characterization of Dissolved Organic Matter in the Ice Shelf Systems of King George Island, Antarctica. Front Mar Sci 7: 339.

KAHRU M, MITCHELL BG, GILLE ST, HEWES CD & HOLM-HANSEN O. 2007. Eddies enhance biological production in the Weddell-Scotia Confluence of the Southern Ocean. Geophys Res Lett 34: L14603.

KERR R, DOTTO TS, MATA MM & HELLMER HH. 2018a. Three decades of deep water mass investigation in the Weddell Sea (1984-2014): Temporal variability and changes. Deep Sea Res 2 Top Stud Oceanogr 149: 70-83.

KERR R, MATA MM, MENDES CRB & SECCHI ER. 2018b. Northern Antarctic Peninsula: a marine climate hotspot of rapid changes on ecosystems and ocean dynamics. Deep Sea Res 2 Top Stud Oceanogr 149: 4-9.

LOEB V, HOFMANN EE, KLINCK JM & HOLM-HANSEN O. 2010. Hydrographic control of the marine ecosystem in the South Shetland-Elephant Island and Bransfield Strait region. Deep Sea Res 2 Top Stud Oceanogr 57: 519-542.

LOEB VJ, HOFMANN EE, KLINCK JM, HOLM-HANSEN O & WHITE WB. 2009. ENSO and variability of the antarctic peninsula pelagic marine ecosystem. Antarct Sci 21: 135-148.

LOGINOVA AN, THOMSEN S, DENGLER M, LÜDKE J & ENGEL A. 2018. Diapycnal dissolved organic matter supply into the upper Peruvian oxycline. Biogeosciences 16: 2033-2047.

LØNBORG C, CARREIRA C, JICKELLS T & ÁLVAREZ-SALGADO XA. 2020. Impacts of Global Change on Ocean Dissolved Organic Carbon (DOC) Cycling. Front Mar Sci 7: 466.

LOPEZ CN & HANSELL DA. 2023. Anomalous DOC signatures reveal iron control on export dynamics in the Pacific Southern Ocean. Front Mar Sci 10: 1070458.

LOVECCHIO E, CLÉMENT L, EVANS C, RAYNE R, DUMOUSSEAUD C, ROSHAN S, GIERING SLC & MARTIN A. 2023. Export of Dissolved Organic Carbon (DOC) compared to the particulate and active fluxes near South Georgia, Southern Ocean. Deep Sea Res 2 Top Stud Oceanogr 212: 105338.

MATA MM, TAVANO VM & GARCIA CAE. 2018. 15 years sailing with the Brazilian High Latitude Oceanography Group (GOAL). Deep Sea Res 2 Top Stud Oceanogr 149: 1-3.

MENDES CRB, DE SOUZA MS, GARCIA VMT, LEAL MC, BROTAS V & GARCIA CAE. 2012. Dynamics of phytoplankton communities during late summer around the tip of the Antarctic Peninsula. Deep Sea Res 1 Oceanogr Res Pap 65: 1-14.

MENDES CRB, TAVANO VM, DOTTO TS, KERR R, DE SOUZA MS, GARCIA CAE & SECCHI ER. 2018. New insights on the dominance of cryptophytes in Antarctic coastal waters: A case study in Gerlache Strait. Deep Sea Res 2 Top Stud Oceanogr 149: 161-170.

MONTEIRO T, HENLEY SF, POLLERY RCG, MENDES CRB, MATA M, TAVANO VM, GARCIA CAE & KERR R. 2023. Spatiotemporal variability of dissolved inorganic macronutrients along the northern Antarctic Peninsula (1996-2019). Limnol Oceanogr 68: 2305-2326.

MONTEIRO T, KERR R, ORSELLI IBM & LENCINA-AVILA JM. 2020. Towards an intensified summer CO2 sink behaviour in the Southern Ocean coastal regions. Prog Oceanogr 183: 102267.

OGAWA H, FUKUDA R & KOIKE I. 1999. Vertical distributions of dissolved organic carbon and nitrogen in the Southern Ocean. Deep Sea Res 1 Oceanogr Res Pap 46: 1809-1826.

OGAWA H & TANOUE E. 2003. Dissolved Organic Matter in Oceanic Waters. J Oceanogr 59: 129-147.

ORELLANA MV & VERDUGO P. 2003. Ultraviolet radiation blocks the organic carbon exchange between the dissolved phase and the gel phase in the ocean. Limnol Oceanogr 48: 1618-1623.

ORSI AH, WHITWORTH T & NOWLIN WD. 1995. On the meridional extent and fronts of the Antarctic Circumpolar Current. Deep Sea Res 1 Oceanogr Res Pap 42: 641-673.

REINTHALER T, ÁLVAREZ SALGADO XA, ÁLVAREZ M, VAN AKEN HM & HERNDL GJ. 2013. Impact of water mass mixing on

the biogeochemistry and microbiology of the Northeast Atlantic Deep Water. Global Biogeochem Cycles 27: 1151-1162.

ROMERA-CASTILLO C, ÁLVAREZ M, PELEGRÍ JL, HANSELL DA & ÁLVAREZ-SALGADO XA. 2019. Net Additions of Recalcitrant Dissolved Organic Carbon in the Deep Atlantic Ocean. Global Biogeochem Cycles 33: 1162-1173.

ROMERA-CASTILLO C, LETSCHER RT & HANSELL DA. 2016. New nutrients exert fundamental control on dissolved organic carbon accumulation in the surface Atlantic Ocean. Proc Natl Acad Sci U S A 113: 10497-10502.

ROSHAN S & DEVRIES T. 2017. Efficient dissolved organic carbon production and export in the oligotrophic ocean. Nat Commun 8: 2036.

RUIZ BARLETT EM, TOSONOTTO GV, PIOLA AR, SIERRA ME & MATA MM. 2018. On the temporal variability of intermediate and deep waters in the Western Basin of the Bransfield Strait. Deep Sea Res 2 Top Stud Oceanogr 149: 31-46.

RUIZ-HALPERN S, CALLEJA ML, DACHS J, DEL VENTO S, PASTOR M, PALMER M, AGUSTÍ S & DUARTE CM. 2014. Ocean-atmosphere exchange of organic carbon and CO2 surrounding the Antarctic Peninsula. Biogeosciences 11: 2755-2770.

RUIZ-HALPERN S, DUARTE CM, TOVAR-SANCHEZ A, PASTOR M, HORSTKOTTE B, LASTERNAS S & AGUSTIÁ S. 2011. Antarctic krill as a source of dissolved organic carbon to the Antarctic ecosystem. Limnol Oceanogr 56: 521-528.

SANGRÀ P, GORDO C, HERNÁNDEZ-ARENCIBIA M, MARRERO-DÍAZ A, RODRÍGUEZ-SANTANA A, STEGNER A, MARTÍNEZ-MARRERO A, PELEGRÍ JL & PICHON T. 2011. The Bransfield current system. Deep Sea Res 1 Oceanogr Res Pap 58: 390-402.

SANGRÀ P, STEGNER A, HERNÁNDEZ-ARENCIBIA M, MARRERO-DÍAZ Á, SALINAS C, AGUIAR-GONZÁLEZ B, HENRÍQUEZ-PASTENE C & MOURIÑO-CARBALLIDO B. 2017. The Bransfield Gravity Current. Deep Sea Res 1 Oceanogr Res Pap 119: 1-15.

SANTINELLI C, IACONO R, NAPOLITANO E & RIBERA D'ALCALÁ M. 2021. Surface transport of DOC acts as a trophic link among Mediterranean sub-basins. Deep Sea Res 1 Oceanogr Res Pap 170: 103493.

SANTOS-ANDRADE M, KERR R, ORSELLI IBM, MONTEIRO T, MATA MM & GOYET C. 2023. Drivers of Marine CO2-Carbonate Chemistry in the Northern Antarctic Peninsula. Global Biogeochem Cycles 37: e2022GB007518.

SCHAFSTALL J, DENGLER M, BRANDT P & BANGE H. 2010. Tidal-induced mixing and diapycnal nutrient fluxes in the Mauritanian upwelling region. J Geophys Res Oceans 115: C10014.

SCHLITZER R. 2024. Ocean Data View. Available at: https://odv.awi.de.

SIGNORI CN, PELLIZARI VH, ENRICH-PRAST A & SIEVERT SM. 2018. Spatiotemporal dynamics of marine bacterial and archaeal communities in surface waters off the northern Antarctic Peninsula. Deep Sea Res 2 Top Stud Oceanogr 149: 150-160.

SIGNORI CN, THOMAS F, ENRICH-PRAST A, POLLERY RCG & SIEVERT SM. 2014. Microbial diversity and community structure across environmental gradients in Bransfield Strait, Western Antarctic Peninsula. Front Microbiol 5: 647.

SU Z, ZHANG Z, ZHU Y & ZHOU M. 2022. Long-Term Warm-Cold Phase Shifts in the Gerlache Strait, Western Antarctic Peninsula. Front Mar Sci 9: 877043.

TESTA G, PIÑONES A & CASTRO LR. 2021. Physical and Biogeochemical Regionalization of the Southern Ocean and the CCAMLR Zone 48.1. Front Mar Sci 8: 592378.

VERA CS & OSMAN M. 2018. Activity of the Southern Annular Mode during 2015-2016 El Niño event and its impact on Southern Hemisphere climate anomalies. Int J Climatol 38: e1288-e1295.

VETROV A & ROMANKEVICH E. 2019. Distribution and fluxes of dissolved organic carbon in the arctic ocean. Polar Res 38: 3500.

WARD P ET AL. 2002. The Southern Antarctic Circumpolar Current Front: physical and biological coupling at South Georgia. Deep Sea Res 1 Oceanogr Res Pap 49: 2183-2202.

WIEBINGA CJ & DE BAAR HJW. 1998. Determination of the distribution of dissolved organic carbon in the Indian sector of the Southern Ocean. Mar Chem 61: 185-201.

ZHANG JZ, BARINGER MO, FISCHER CJ & HOOPER VJA. 2017. An estimate of diapycnal nutrient fluxes to the euphotic zone in the Florida Straits. Sci Rep 7: 16098.

ZHOU M, NIILER PP & HU J-H. 2002. Surface currents in the Bransfield and Gerlache Straits, Antarctica. Deep Sea Res 1 Oceanogr Res Pap 49: 267-280.

How to cite

AVELINA R, DA CUNHA LC, KERR R, FARIAS CO, HAMACHER C & MATA MM. 2024. Drivers and fluxes of dissolved organic carbon along the northern Antarctic Peninsula during late summer. An Acad Bras Cienc 96: e20240573. DOI 10.1590/0001-3765202420240573.

Manuscript received on May 29, 2024;
accepted for publication on September 10, 2024

RAQUEL AVELINA[1,2,3]
https://orcid.org/0000-0002-8283-2104

LETICIA C. DA CUNHA[1,2,3,4]
https://orcid.org/0000-0001-8035-1430

RODRIGO KERR[3,5,6]
https://orcid.org/0000-0002-2632-3137

CÁSSIA O. FARIAS[1,7]
https://orcid.org/0000-0003-4578-0883

CLAUDIA HAMACHER[1,7]
https://orcid.org/0000-0002-4807-3247

MAURICIO M. MATA[5,6]
https://orcid.org/0000-0002-9028-8284

[1]Universidade do Estado do Rio de Janeiro, Programa de Pós-Graduação em Oceanografia, Rua São Francisco Xavier, 524, 4018E, Pav. João Lyra, Campus Maracanã, 20550-900 Rio de Janeiro, RJ, Brazil

[2]Universidade do Estado do Rio de Janeiro, Faculdade de Oceanografia, Laboratório de Oceanografia Química, Rua São Francisco Xavier, 524, 4018E, Pav. João Lyra, Campus Maracanã, 20550-900 Rio de Janeiro, RJ, Brazil

[3]Brazilian Ocean Acidification Network (BrOA), Av. Itália, s/n, 96203-900 Rio Grande, RS, Brazil

[4]Instituto Nacional de Pesquisas Espaciais (INPE), Rede Clima, Subrede Oceanos, Av. dos Astronautas, 1758, 12227-010 São José dos Campos, SP, Brazil

[5]Universidade Federal do Rio Grande (FURG), Instituto de Oceanografia, Laboratório de Estudos dos Oceanos e Clima, Av. Itália, s/n, 96203-900 Rio Grande, RS, Brazil

[6]Universidade Federal do Rio Grande (FURG), Programa de Pós-Graduação em Oceanologia, Instituto de Oceanografia, Av. Itália, s/n, 96203-900 Rio Grande, RS, Brazil

[7]Universidade do Estado do Rio de Janeiro, Faculdade de Oceanografia, Laboratório de Geoquímica Orgânica Marinha, Rua São Francisco Xavier, 524, 4018E, Pav. João Lyra, Campus Maracanã, 20550-900 Rio de Janeiro, RJ, Brazil

Correspondence to: **Raquel Avelina**
E-mail: santos.raquel@posgraduacao.uerj.br

Author contributions

R. Avelina: Conceptualization, Field work, Formal analysis, Investigation, Methodology, Data Curation, Writing. L.C. da Cunha: Conceptualization, Field work, Investigation, Supervision, Data Curation and Quality Control, Writing. R. Kerr: Field work, Investigation, Data Curation and Quality Control, Funding Acquisition, Project administration, Writing. C.O. Farias: Formal analysis, Data Curation and Quality control, Writing. C. Hamacher: Formal analysis, Data Curation and Quality control, Writing. M.M. Mata: Investigation, Funding Acquisition, Project administration, Writing.